

Hesperetin reverses P-glycoprotein-mediated cisplatin resistance in DDP-resistant human lung cancer cells via modulation of the nuclear factor- κ B signaling pathway

WENCUI KONG^{1*}, XIAOMING LING^{2*}, YING CHEN^{1*}, XIAOLI WU¹, ZHONGQUAN ZHAO¹, WENWU WANG³, SHUILIANG WANG^{4,5}, GUOXIANG LAI⁶ and ZONGYANG YU^{1,7-9}

¹Department of Medical Oncology, 900 Hospital of The Joint Logistics Team, Fuzhou, Fujian 350025;

²Faculty of Rehabilitation Medicine, Fujian University of Traditional Chinese Medicine, Fuzhou, Fujian 350122;

³Department of Medical Oncology, The Third Affiliated People's Hospital of Fujian University of Traditional Chinese Medicine, Fuzhou, Fujian 350108; ⁴Department of Urology, 900th Hospital of The Joint Logistics Team, Fujian Medical University, Fuzhou, Fujian 350025; ⁵Fujian Key Laboratory of Transplant Biology, Affiliated Dongfang Hospital, Xiamen University School of Medicine, Xiamen, Fujian 361102;

⁶Department of Respiratory and Critical Care Medicine, 900 Hospital of The Joint Logistics Team;

⁷Fujian Medical University Affiliated Dongfang Hospital, Fuzhou, Fujian 350025; ⁸Xiamen University School of Medicine, Xiamen, Fujian 361102; ⁹Fujian University of Traditional Chinese Medicine, Fuzhou, Fujian 350122, P.R. China

Received August 3, 2019; Accepted January 10, 2020

DOI: 10.3892/ijmm.2020.4485

Abstract. Lung cancer is the leading cause of cancer-associated mortality worldwide. Cisplatin (DDP) is a first-line chemotherapeutic drug for the treatment of lung cancer; however, the majority of patients develop resistance to DDP. P-glycoprotein (P-gp), also referred to as multidrug resistance (MDR) protein 1, is associated with an MDR phenotype, which results in failure of cancer chemotherapy; thus, identifying effective MDR pump inhibitors may improve the outcomes of patients who develop resistance to treatment. Hesperetin is a derivative of hesperidin, which is extracted from tangerine peel and exhibits multiple antitumor properties. In the present study, human lung adenocarcinoma A549 and A549/DDP cells were treated with different concentrations of hesperetin and DDP, respectively. Furthermore, rhodamine 123 efflux assays, Cell Counting Kit-8 assays, immunofluorescence, reverse transcription-quantitative PCR and western blot analysis were used to elucidate the mechanisms underlying the effects of hesperetin on A549/DDP cells. Additionally, a xenograft model of lung cancer in nude mice was established to explore

the effects of hesperetin on A549/DDP cell growth *in vivo*. The results demonstrated that hesperetin sensitized A549/DDP cells to DDP. *In vivo*, hesperetin pretreatment significantly inhibited tumor growth. Mechanistically, hesperetin markedly decreased the expression of P-gp and increased the intracellular accumulation of the P-gp substrate, rhodamine 123, in A549/DDP cells. In addition, pretreatment of A549/DDP cells with hesperetin significantly inhibited nuclear factor (NF)- κ B (p65) activity and its nuclear translocation. Taken together, the results of the present study suggest that hesperetin reversed P-gp-mediated MDR by decreasing P-gp expression in A549/DDP cells, which was associated with inhibition of the NF- κ B signaling pathway. These findings may provide the basis for the use of hesperetin clinically to reverse MDR.

Introduction

Lung cancer is the most common type of malignant tumor, with the highest morbidity and mortality rates globally, resulting in >100,000 deaths annually (1). Pathologically, lung cancer is classified into two broad subgroups, namely small-cell lung cancer and non-small-cell lung cancer (NSCLC), with NSCLC accounting for 85% of all cases (2,3). Patients with early-stage lung cancer are often asymptomatic and, thus, are often first diagnosed with advanced-stage lung cancer, at which point resection of the tumor may not be possible; therefore, patients with advanced-stage lung cancer are most frequently treated with chemotherapy or radiotherapy (4-6). Cisplatin (DDP) is a first-line chemotherapeutic for lung cancer (7). DDP-DNA cross-linking prevents DNA replication, resulting in apoptosis of lung cancer cells (8,9). However, patients frequently develop resistance to chemotherapy (10-12). Therefore, identifying therapeutics that can reverse drug resistance by enhancing

Correspondence to: Professor Zongyang Yu, Department of Medical Oncology, 900 Hospital of The Joint Logistics Team, 156 Xi'erhuan North Road, Fuzhou, Fujian 350025, P.R. China
E-mail: yuzongyang156@163.com

*Contributed equally

Key words: hesperetin, P-glycoprotein, nuclear factor- κ B signaling pathway, drug resistance, lung cancer

the sensitivity of tumor cells to drugs, thereby reducing the concentration of drugs used, may improve the outcomes of patients.

Herbal/botanical-based medicines have been intensively studied for several decades, as some exert beneficial effects when used to treat several different diseases (13,14), including various types of cancer (15,16). Hesperidin and the hesperidin derivative hesperetin possess various beneficial biological properties (17). Hesperidin inhibits proliferation and induces apoptosis in lung cancer cells, without notable toxic effects on normal lung epithelial cells (18). Furthermore, hesperidin inhibits the migration and invasion of lung cancer cells by regulating the SDF1/CXCR4 axis (19). *In vivo*, hesperidin pretreatment protects against the development of carcinogen-induced lung cancer from multiple carcinogens (20-23).

Hesperetin, the glycoside ligand derivative of hesperidin, exhibits good bioavailability (24). It has been demonstrated that hesperetin prevented 1,2-dimethylhydrazine-induced colorectal cancer (25,26) and induced apoptosis of colorectal cancer cells in a dose-dependent manner (27). The aim of the present study was to investigate the effects of hesperetin treatment on the sensitivity of A549/DDP cells to certain drugs. Understanding the molecular mechanism of action of hesperetin in the drug resistance of tumor cells may provide the basis for the use of hesperetin as an adjuvant to prevent multidrug resistance (MDR) in the clinical setting.

Materials and methods

Cell culture. Human lung cancer A549 and A549/DDP cells were obtained from The Cell Bank of Type Culture Collection of the Chinese Academy of Sciences and cultured with RPMI-1640 medium containing 10% FBS (both from HyClone; GE Healthcare) and 1% penicillin-streptomycin (Gibco; Thermo Fisher Scientific, Inc.) with a 5% CO₂ atmosphere at 37°C.

Preparation of hesperetin, DDP and JSH-23 solutions. Hesperetin powder (Sigma-Aldrich; Merck KGaA) was dissolved in DMSO and diluted to 0.6, 1.25, 2.5, 5, 10, 20, 40, 80 and 160 µM using RPMI-1640 medium. DDP was dissolved in sterile PBS to 1 mg/ml, and subsequently diluted to 0.6, 1.25, 2.5, 5, 10, 20, 40, 80 and 160 µg/ml using culture medium. The nuclear factor (NF)-κB signaling pathway inhibitor JSH-23 (Sigma-Aldrich; Merck KGaA) was dissolved in DMSO and diluted to 1 µM.

Cell counting kit-8 (CCK-8) assay. A549 and A549/DDP cells were seeded into 96-well plates at a density of 1x10⁴ cells/well and treated with hesperetin, alone or in combination with DDP, for 72 h. The medium was removed, and the cells were incubated with 10% CCK-8 reagent for 2 h at 37°C. Absorbance values were measured at 450 nm using an enzyme-labeling instrument (iMARK, Bio-Rad Laboratories, Inc.). Experiments were performed in triplicates.

Flow cytometry. A549/DDP cells were seeded into 6-well plates at a density of 8x10⁵ cells/well and treated with 1.25, 2.5, 5 and 10 µM hesperetin for 72 h. Subsequently, 50 µg/ml DDP was added and the cells were further incubated for 48 h. Cells

treated with 50 µg/ml DDP were used as a positive control. Untreated cells served as the negative control. Subsequently, cells were collected and stained using an Annexin V-FITC/PI kit (cat. no. CA1020; Beijing Solarbio Science & Technology Co., Ltd.) according to the manufacturer's instructions. The proportion of apoptotic cells was analyzed using flow cytometry (BD Biosciences). Analysis of apoptosis was performed by FlowJo 7.6 software (Becton, Dickinson and Company). Experiments were performed in triplicates.

Reverse transcription-quantitative PCR (RT-qPCR) analysis. A549/DDP cells were seeded in 6-well plates at a density of 8x10⁵ cells/well and treated with hesperetin or DDP for 72 h, as described above. Cells were harvested and total RNA was extracted using TRIzol[®] reagent, according to the manufacturer's protocol (Thermo Fisher Scientific, Inc.). The purity and concentration of the extracted total RNA were measured using an ultraviolet spectrophotometer, and an A260/A280 value of 1.8-2 was considered acceptable. A total of 1 µg RNA was reverse-transcribed into cDNA according to the manufacturer's protocol. The reverse transcription conditions were 37°C for 15 min; 85°C for 5 sec; and held at 4°C. Reverse transcription and SYBR-Green qPCR kits were obtained from Beijing Transgen Biotech Co., Ltd. qPCR primers were purchased from Sangon Biotech Co., Ltd. Subsequently, using cDNA as a template and β-actin as an internal reference, the relative expression was determined using an ABI7500 Real Time PCR system (Thermo Fisher Scientific, Inc.). The thermocycling conditions were as follows: Pre-denaturation at 95°C for 5 min, followed by 40 cycles of denaturation at 95°C for 15 sec and annealing at 60°C for 15 sec. qPCR was performed in triplicates, and the relative expression levels of the target genes were calculated using the 2^{-ΔΔC_q} method (28). All reactions were performed in triplicate. The sequences of the primers used were as follows: P-glycoprotein (P-gp) forward, TTGCTGCTTACATTCAGGTTTCA and reverse, AGCCTATCTCCTGTGCATTA; epidermal growth factor receptor-2 (c-erbB-2) forward, TGTGACTGCCTGTCCCTCAA and reverse, CCAGACCATAGCACACTCGG; glutathione s-transferase (GST-π) forward, TTGGGCTCTATGGGAAGGAC and reverse, GGGAGATGTATTTGCAGCGGA; and β-actin forward, CCTCGCCTTTGCCGATCC and reverse, GGATCTTCATGAGGTAGTCAGTC.

Western blotting. After A549/DDP cells were treated with hesperetin for 72 h, and total protein was extracted using ice-cold RIPA lysis buffer (Beyotime Institute of Biotechnology). The protein concentration of each group was determined using a bicinchoninic acid assay. Proteins (30 µg per lane) were loaded on a 10% SDS-gel, resolved using SDS-PAGE, transferred to PVDF membranes (EMD Millipore) and subsequently blocked with 5% skimmed milk for 2 h at room temperature. Membranes were probed with one of the following primary antibodies: Rabbit anti-P-gp (1:1,000; cat. no. ab129450; Abcam), mouse anti-IκB (1:1,000; cat. no. sc-1643; Santa Cruz Biotechnology, Inc.), mouse anti-phosphorylated (p-)IκB (1:1,000; cat. no. sc-8404; Santa Cruz Biotechnology, Inc.), rabbit anti-NF-κB p65 (1:1,000; cat. no. ab16502; Abcam), rabbit anti-NF-κB p65 (p-S536) (1:1,000; cat. no. ab28856; Abcam), rabbit anti-histone H3 anti-

body (1:2,000; cat. no. ab201456; Abcam) or rabbit anti-human β -actin primary antibody (1:4,000; cat. no. ab179467; Abcam), overnight at 4°C. Subsequently, the membranes were incubated with a horseradish peroxidase-conjugated goat anti-rabbit antibody (cat. no. ab6721; Abcam) or horseradish peroxidase-conjugated goat anti-mouse antibody (cat. no. ab6789; Abcam) both at 1:5,000 at room temperature for 3 h. Signals were visualized with enhanced chemiluminescence solution (EMD Millipore) and developed using chemiluminescence apparatus (GE Healthcare). Densitometry analysis was performed using Quantity One, version 4.6.7 (Bio-Rad Laboratories, Inc.). Experiments were repeated three times.

Preparation of nuclear and cytosolic extracts. A nucleoprotein separation kit (NE-PER™ Nuclear and Cytoplasmic Extraction Reagents) was purchased from Thermo Fisher Scientific, Inc. (cat. no. 78833). Nuclear and cytosolic extracts were prepared according to manufacturer's protocol. All steps were performed on ice or at 4°C. Briefly, A549/DDP cells were seeded in 6-well plates at a density of 8×10^5 cells per well and treated with hesperetin for 72 h as described above. After digesting, re-suspending and centrifuging at $500 \times g$ for 4 min at 4°C, the cells were incubated in CER I on ice for 10 min and pre-cooled CER II was added for 1 min. The supernatant (cytosolic extract) was collected by centrifugation at $15,000 \times g$ for 10 min at 4°C. Subsequently, the insoluble compounds were immersed in NER on ice for 40 min, and centrifuged at $15,000 \times g$ for 10 min at 4°C. The supernatant was the nuclear extract and was analyzed by western blotting. Experiments were repeated three times independently.

Immunofluorescence. A549/DDP cells were seeded at a density of 1×10^5 cells/well in a 6-well plate preloaded with sterile glass coverslips. After treatment with hesperetin for 72 h, cell slides were removed and fixed with 4% paraformaldehyde for 15 min at room temperature, and permeabilized with 0.25% Triton for 10 min and blocked with 5% BSA for 1 h. Subsequently, cells were incubated with 5% BSA-diluted rabbit anti-NF- κ B p65 antibody (1:300; cat. no. ab16502; Abcam) or mouse anti-P-gp antibody (1:300; cat. no. ab80594; Abcam) overnight at 4°C, followed by incubation with 5% BSA-diluted goat anti-mouse IgG H&L (Alexa Fluor® 555; 1:300; cat. no. ab150078; Abcam) or goat anti-rabbit IgG H&L (Alexa Fluor® 488; 1:300; cat. no. ab150077; Abcam) for 2 h at room temperature. Finally, nuclei were stained with DAPI (1:10,000; Beyotime Institute of Biotechnology, Inc.) for 5 min at room temperature and imaged immediately using a fluorescence microscope (magnification, $\times 200$; Olympus Corporation). Experiments were repeated three times.

Rhodamine 123 efflux assay to assess P-gp function. A549/DDP cells were plated at a density of 8×10^5 cells/well in 6-well plates and treated with hesperetin for 72 h. Untreated cells were used as the control. Subsequently, the cells were stained with 5 μ g/ml rhodamine 123 (Santa Cruz Biotechnology, Inc.), followed by incubation at 37°C in 5% CO₂ for 1 h. The cells were centrifuged at $400 \times g$ for 5 min at room temperature, washed twice with medium and re-suspended. The fluorescence value was analyzed by flow cytometry at an excitation/emission wavelength of 488/530 nm. Experiments were performed in triplicates.

Xenograft experiments. Five-week-old nude mice were maintained and handled according to the instructions approved by the Animal Care Committee of 900 Hospital of the Joint Logistics Team. A549/DDP cells at the logarithmic growth phase were collected and adjusted to a density of 5×10^7 cells/ml. Nude mice were randomly divided into three groups: Control, DDP-treated and co-treated with DDP and hesperetin, with 6 mice in each group. The cells (5×10^6 cells in 0.1 ml) were subcutaneously injected in the right armpit of the nude mice. Mice in the co-treatment group were intragastrically administered 2 mg/kg hesperetin every 2 days. Mice in the control and DDP treatment groups were administered PBS. The diameter of the subcutaneous tumor was measured every 4 days. After 3 weeks, when the mean tumor diameter reached 5 mm, the DDP-treated and the co-treatment groups were administered 2 mg/kg DDP every 2 days intraperitoneally. The control group mice were injected with an equivalent volume of PBS. When the maximum tumor diameter exceeded 12 mm (52 days after subcutaneous injection), the nude mice were sacrificed by cervical dislocation, and tumor volume was measured. All mouse experiments were approved by the Animal Care and Use Committee of 900 Hospital of the Joint Logistics Team and carried out in accordance with the Guide for the Care and Use of Laboratory Animals.

Statistical analysis. Data were analyzed and graphing was performed using SPSS, version 21.0 (IBM Corp.) and GraphPad Prism, version 6.0 (GraphPad Software, Inc.), respectively. Statistical results are presented as the mean \pm standard deviation. Differences between multiple groups were compared using one-way ANOVA with a post-hoc Dunnett's test (when all groups are compared with the control group) or Bonferroni test (when all groups are compared). Differences between two groups were analyzed using Student's t-test. $P < 0.05$ was considered to indicate a statistically significant difference.

Results

Toxic effects of different concentrations of hesperetin on parental A549 cells and DDP-resistant (A549/DDP) cells. As shown in Fig. 1, compared with the matched control group, low concentrations of hesperetin ($< 5 \mu$ M) exerted no effect on A549 and A549/DDP cells ($P > 0.05$). In addition, low concentrations of DDP ($< 5 \mu$ M) had no effect on A549/DDP cells ($P > 0.05$). Higher concentrations ($> 20 \mu$ M) of hesperetin and DDP significantly reduced the proliferation of both types of cells in a dose-dependent manner ($P < 0.05$). Furthermore, there was no significant difference in the IC₅₀ values between these two types of cells treated with hesperetin ($P > 0.05$), whereas the IC₅₀ values differed significantly between DDP-treated A549 and A549/DDP cells (6.28 ± 1.39 vs. $78.3 \pm 4.31 \mu$ g/ml, respectively; $P < 0.05$).

Hesperetin pretreatment exerts a synergistic effect on A549/DDP cells. To determine whether hesperetin improved the sensitivity of A549/DDP cells to DDP, cells were treated with hesperetin either alone or combined with DDP. Cells were treated with different concentrations of hesperetin (0.6, 1.25, 2.5, 5 or 10 μ M) for 72 h, and subsequently incubated with different concentrations of DDP (10, 20, 40 or 80 μ g/ml)

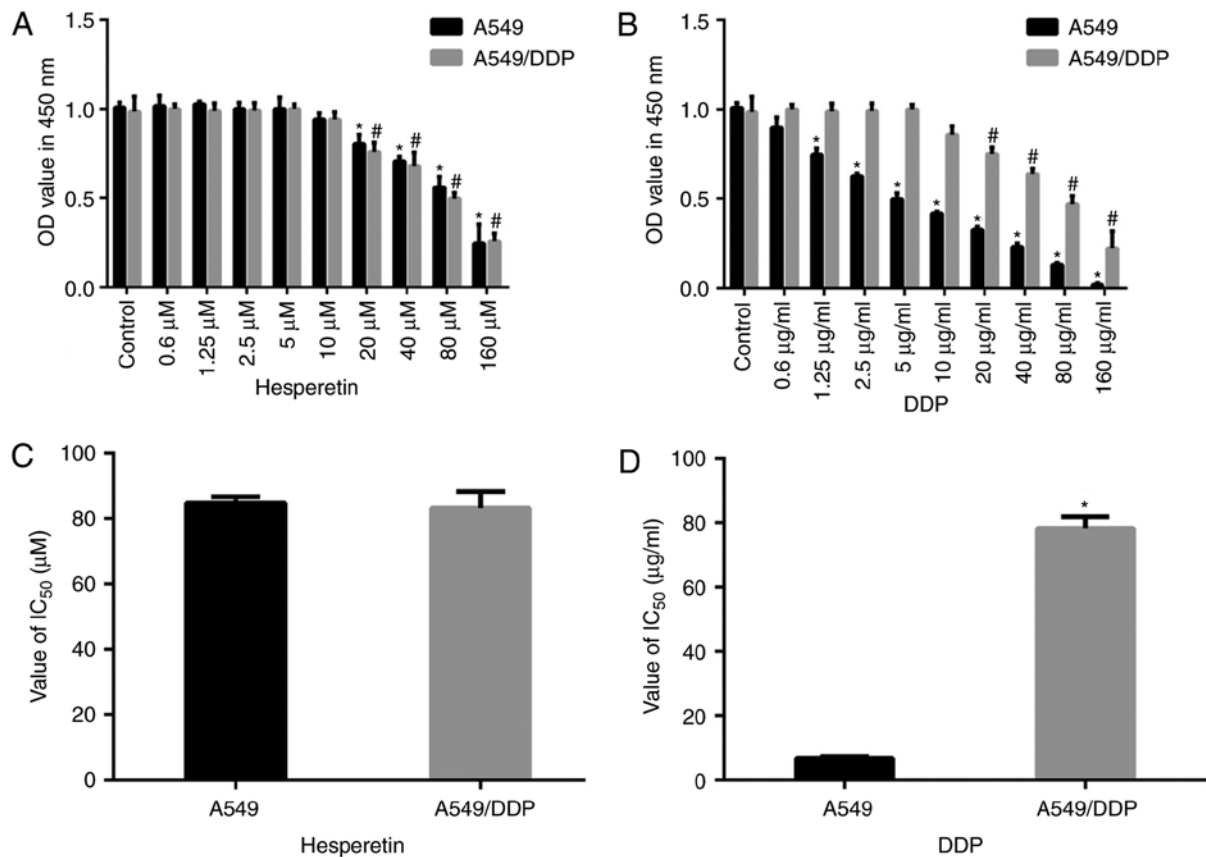


Figure 1. Toxicity of hesperetin and DDP in A549 and A549/DDP cells. (A) Effects of various concentrations of hesperetin on the viability of A549 and A549/DDP cells. (B) Effects of various concentrations of DDP on the viability of A549 and A549/DDP cells. (C) IC_{50} values of hesperetin-treated A549 and A549/DDP cells. (D) DDP significantly increased the IC_{50} values of A549/DDP cells compared with A549 cells. * $P < 0.05$ vs. control (A549 cells). # $P < 0.01$ vs. control (A549/DDP cells). Error bars represent the standard deviations. $n = 3$. DDP, cisplatin; IC_{50} , half-maximal inhibitory concentration; OD, optical density.

for 48 h, or treated with hesperetin and DDP together. Cells treated with DDP alone were used as the control group. Cell viability was measured using CCK-8 assays. When the cells were treated with 0.6 or 1.25 μM hesperetin followed by treatment with various concentrations of DDP, no significant difference was observed among the different groups (Fig. 2). The IC_{50} values of DDP in A549/DDP cells did not differ significantly ($P > 0.05$). However, when the concentration of hesperetin was increased to 2.5, 5 or 10 μM , the effect of DDP on cells was significantly increased. Additionally, the IC_{50} value was significantly decreased compared with the control cells ($P < 0.05$). In the xenograft mouse model, all nude mice received subcutaneous injection of A549/DDP cells, followed by administration of hesperetin. Treatment of mice with hesperetin had no effect on tumor growth; however, hesperetin treatment followed by administration of DDP resulted in a significant reduction in tumor growth in the nude mice compared with DDP treatment alone. The tumor volume was measured 52 days after inoculation, and it was demonstrated that the DDP-treated group exhibited significantly reduced cell proliferation compared with the control group. Furthermore, compared with the DDP-treated group, the tumor volume in the hesperetin and DDP co-treatment group was significantly reduced.

Hesperetin pretreatment increases the proportion of apoptotic cells in DDP-treated A549/DDP cells. To validate the

mechanism by which hesperetin treatment enhances the sensitivity of A549/DDP cells to DDP, cells were treated with different concentrations of hesperetin and subsequently treated with DDP. Cell apoptosis was measured by flow cytometry. Compared with the positive control group, the proportion of apoptotic A549/DDP cells following hesperetin pretreatment was significantly increased (Fig. 3; $P < 0.05$).

Hesperetin decreases the expression of P-gp. To determine the mechanism by which hesperetin enhances the sensitivity of A549/DDP cells to DDP, the expression of P-gp and the drug resistance-associated genes, c-erbB-2 and GST- π , was assessed using RT-qPCR, western blotting and immunofluorescence assays. Hesperetin downregulated the mRNA levels of P-gp ($P < 0.05$), whereas it exerted no effect on the mRNA levels of c-erbB-2 and GST- π ($P > 0.05$; Fig. 4). Western blotting and immunofluorescence analysis also demonstrated that hesperetin significantly decreased the protein expression levels of P-gp ($P < 0.05$).

Hesperetin treatment promotes the accumulation of rhodamine 123 in A549/DDP cells. To elucidate the mechanism by which hesperetin sensitizes A549/DDP cells to DDP, cells were treated with 10 μM hesperetin and stained with rhodamine 123. The fluorescence values of cells incubated with rhodamine alone were significantly higher compared with those of untreated cells ($P < 0.05$; Fig. 5). The fluorescence

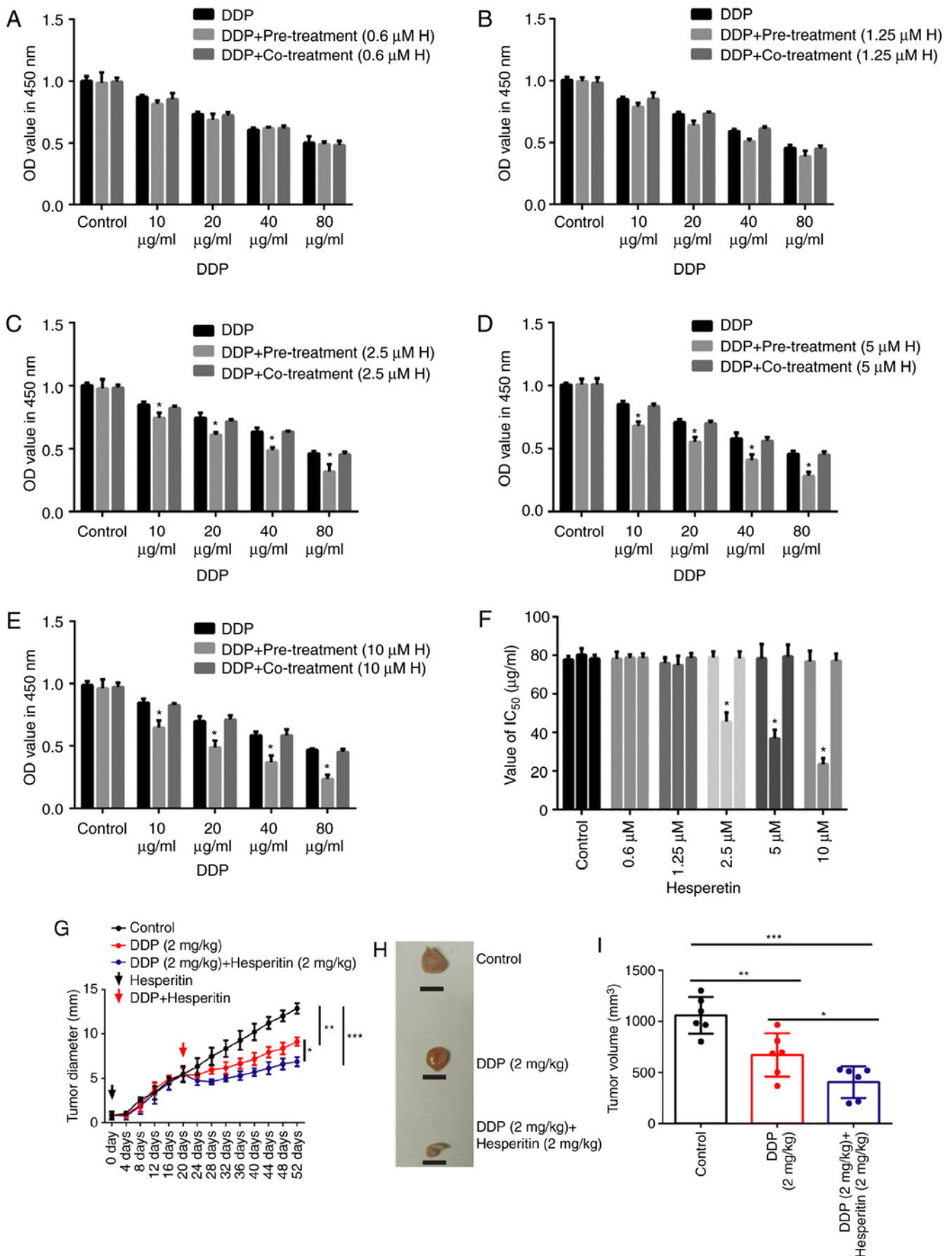


Figure 2. Hesperetin treatment enhances the effects of DDP on A549/DDP cells. Viability of A549/DDP cells incubated with (A) 0.6, (B) 1.25, (C) 2.5, (D) 5 or (E) 10 μM hesperetin for 72 h followed by treatment with different concentrations of DDP for 48 h. (F) IC₅₀ values of cells treated with different concentrations of hesperetin. (G) Tumor diameter in xenograft mice. (H) Representative images of tumors at day 52 and (I) tumor volumes. *P<0.05, **P<0.01, ***P<0.001 vs. control. Error bars represent the standard deviations. n=3. DDP, cisplatin; IC₅₀, half-maximal inhibitory concentration; OD, optical density; H, hesperetin.

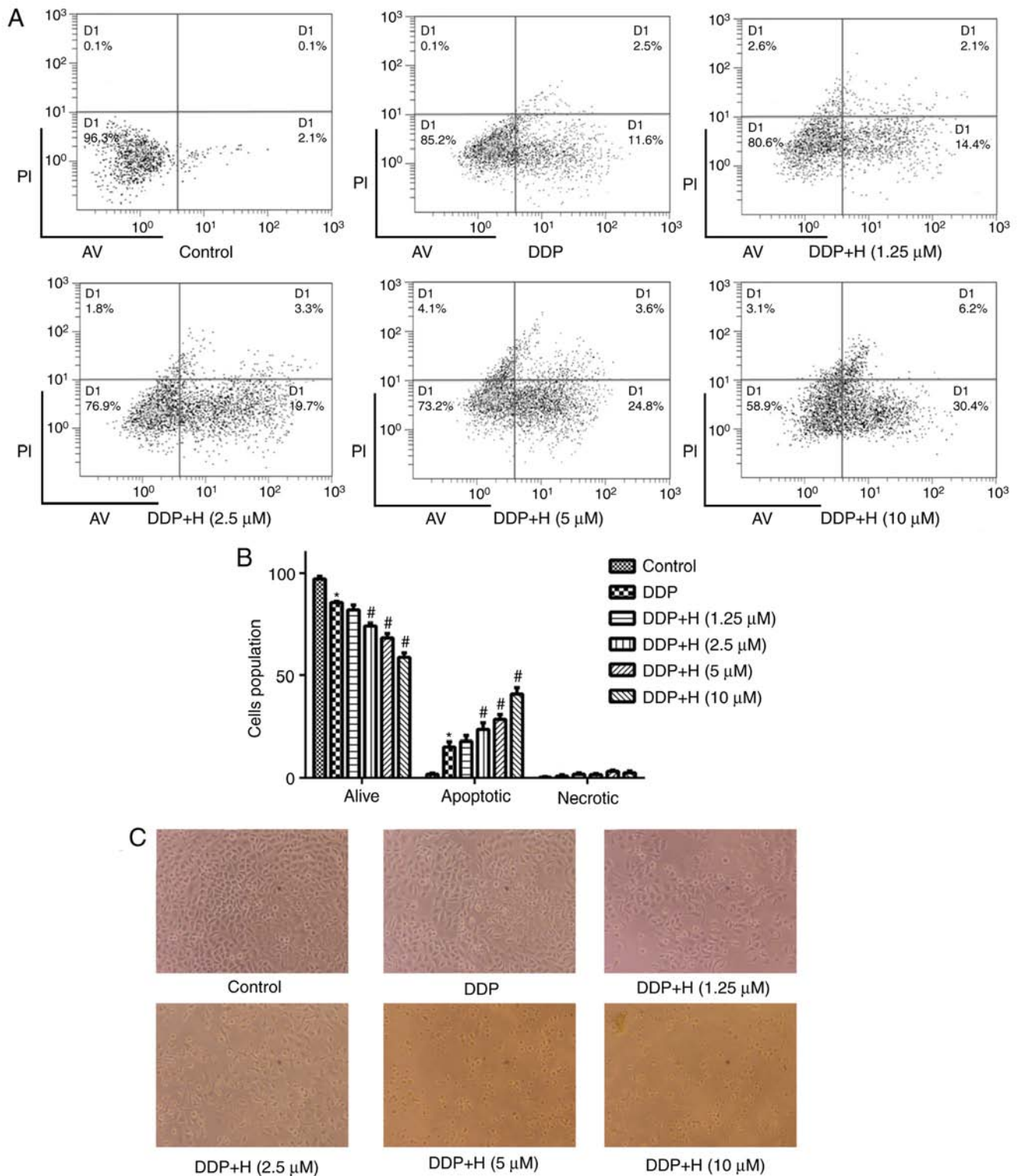


Figure 3. Hesperetin pretreatment increases DDP-induced apoptosis in A549/DDP cells. (A) Representative images of flow cytometry analysis. The proportion of apoptotic cells was relatively low in the negative control group (<5%), whereas in the A549/DDP cells treated with DDP, the proportion was significantly increased. In the cells pretreated with 2.5, 5 or 10 μ M hesperetin, the proportion of apoptotic cells was significantly increased following treatment with DDP. (B) Statistical analysis of the flow cytometry results. (C) Representative images of cells pretreated with different concentrations of hesperetin. Magnification, $\times 200$. * $P < 0.05$ vs. control. # $P < 0.05$ vs. DDP. Error bars represent the standard deviations. $n = 3$. H, hesperetin; DDP, cisplatin; AV, Annexin V; PI, propidium iodide.

values of A549/DDP cells treated with hesperetin were significantly higher compared with those of cells incubated with rhodamine alone ($P < 0.05$), suggesting that hesperetin treatment resulted in an accumulation of rhodamine 123 in A549/DDP cells.

Hesperetin treatment inhibits the activation of the NF- κ B signaling pathway. To verify the mechanism by which hesperetin increases the sensitivity of A549/DDP cells to DDP through downregulation of P-gp expression, A549/DDP cells were treated with various concentrations of hesperetin (1.25,

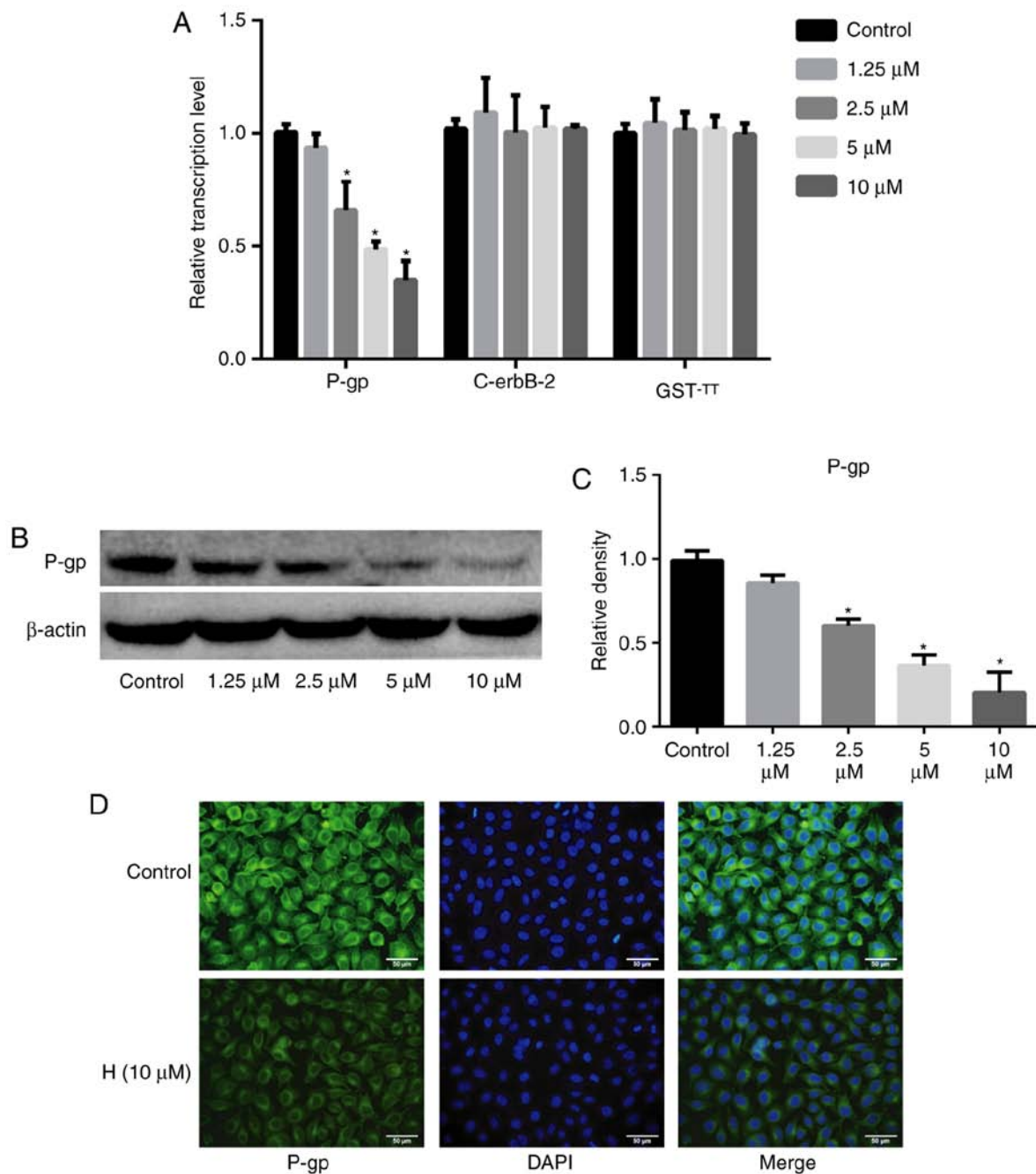


Figure 4. Hesperetin inhibits the expression of P-gp. (A) Effect of different concentrations of hesperetin on the mRNA expression levels of P-gp, c-erbB-2 and GST- π in A549/DDP. Hesperetin significantly downregulated the transcription levels of P-gp, but did not statistically affect the expression levels of c-erbB-2 and GST- π . (B) Representative blots and (C) and densitometry analysis of total P-gp protein expression levels. (D) Immunofluorescence analysis demonstrated that 10 μ M hesperetin significantly downregulated the protein expression levels of P-gp. Magnification, $\times 200$. * $P < 0.05$ vs. control group. Error bars represent the standard deviations. n=3. H, hesperetin; P-gp, P-glycoprotein; c-erbB-2, epidermal growth factor receptor-2; GST- π , glutathione s-transferase.

2.5, 5 or 10 μ M), total protein was extracted, and the expression and activation of NF- κ B signaling pathway-associated proteins were assessed. The intracellular localization of p65 was determined by immunofluorescence. Hesperetin downregulated the phosphorylation of I κ B in a dose-dependent manner ($P < 0.05$), and attenuated the expression of p-p65 ($P < 0.05$); however, it had no significant effect on the expression of total I κ B and total p65 ($P > 0.05$) compared with the control group (Fig. 6). Immunofluorescence revealed that 10 μ M hesperetin could inhibit p65 entry into the nucleus. Extracted cytoplasmic and nuclear proteins were assessed by western blotting and,

compared with the control group, the levels of p65 in the cytoplasm were significantly increased ($P < 0.05$), whereas the levels in the nucleus were significantly decreased ($P < 0.05$) when A549/DDP cells were treated with 10 μ M hesperetin.

Combination treatment with hesperetin and the NF- κ B signaling pathway inhibitor JSH-23 significantly enhances the sensitivity of A549/DDP cells to DDP. The results mentioned above demonstrated that hesperetin attenuated the expression of P-gp by inhibiting the activation of the NF- κ B signaling pathway, thereby increasing the sensitivity

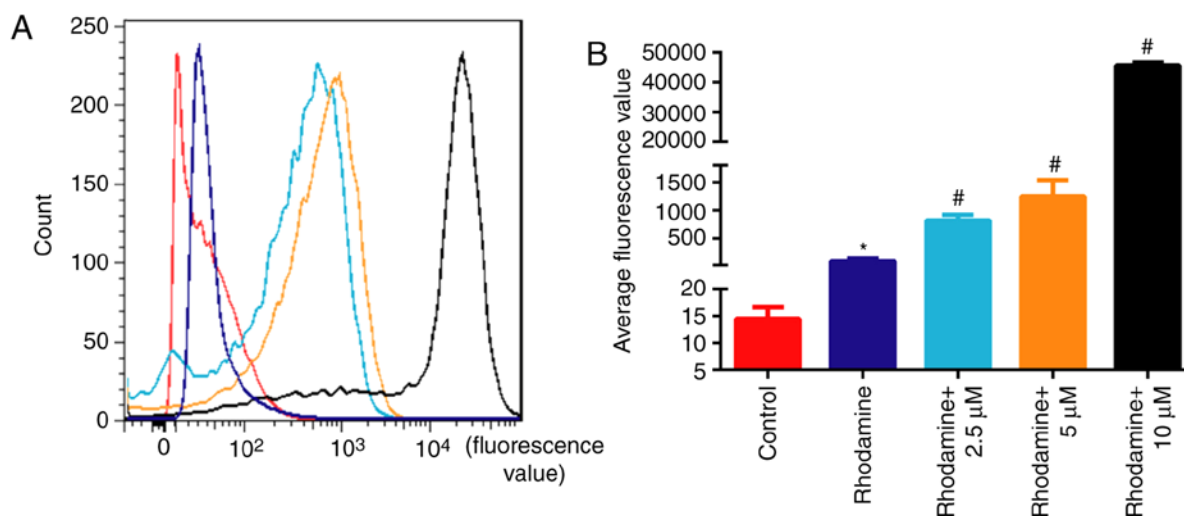


Figure 5. Hesperetin treatment increases intracellular accumulation of rhodamine 123. (A) Rhodamine accumulation in A549/DDP cells treated with different concentrations of hesperetin was detected by flow cytometry, where the fluorescence value represents the content of rhodamine. (B) Quantification of the fluorescence data in (A). * $P < 0.05$ vs. control. # $P < 0.05$ vs. rhodamine. Error bars indicate standard deviations. $n = 3$. DDP, cisplatin.

of A549/DDP cells to DDP. To investigate the therapeutic value of the combination of hesperetin with other therapeutic drugs for the treatment of lung cancer, A549/DDP cells were treated with hesperetin alone or in combination with JSH-23. DDP-treated cells were used as the positive control and untreated cells were used as the negative control. Compared with the negative control group, hesperetin or JSH-23 treatment alone significantly enhanced the effect of DDP on A549/DDP cells ($P < 0.05$; Fig. 7). Furthermore, compared with cells treated with hesperetin or JSH-23 alone, the combination of hesperetin and JSH-23 synergistically improved the effect of DDP on A549/DDP cells ($P < 0.05$), and the IC_{50} values were also notably decreased ($P < 0.05$; Fig. 7). The results of flow cytometry were consistent with those of the CCK-8 assay. Western blotting demonstrated that the combination of hesperetin and JSH-23 significantly attenuated the expression of P-gp ($P < 0.05$; Fig. 7).

Discussion

Despite the rapid development of novel strategies for cancer treatment, DDP remains the most frequently used first-line treatment for patients with lung cancer (7,29). Patients treated with DDP frequently develop resistance, which represents a major clinical challenge. Therefore, compounds that can sensitize patients to chemotherapy or reverse drug resistance may improve patient outcomes. Chinese herbs and their natural extracts have exhibited beneficial anticancer properties by mediating the expression of epithelial-to-mesenchymal transition-associated markers and the expression of genes associated with drug resistance, apoptosis and cell cycle progression (30,31). Tangerine peel is a common Chinese herbal medicine containing a variety of natural compounds, of which hesperidin and its derivative, hesperetin, have exhibited antitumor properties *in vitro* and *in vivo* (19,24,32,33). Hesperetin derived from the catabolism of hesperidin in the intestine has been widely used and investigated (34-36). Previous studies suggested that hesperetin exhibits numerous

beneficial biological functions, including anti-inflammatory and antioxidant properties, and induces apoptosis of tumor cells (37,38). In the present study, hesperetin pretreatment affected the sensitivity of A549/DDP lung cancer cells to DDP; thus, it was hypothesized that hesperetin may sensitize cells to chemotherapy and may be used to reverse drug resistance in patients with lung cancer.

In the present study, A549 and A549/DDP lung cancer cells were treated with various concentrations of hesperetin to determine its toxicity using a proliferation assay, and it was demonstrated that it did not exert any toxic effects on cells when used at $< 10 \mu\text{M}$; therefore, $< 10 \mu\text{M}$ hesperetin was used for all subsequent experiments to avoid its effects on cell proliferation and apoptosis. When hesperetin was used at 0.6 and $1.25 \mu\text{M}$, it did not result in increased cell death when combined with DDP in A549/DDP cells. When increasing the concentration of hesperetin to 2.5, 5 or $10 \mu\text{M}$, the effects were significantly improved. *In vivo*, tumor growth in xenograft mouse models treated with hesperetin resulted in significantly smaller tumors. Thus, it was preliminarily suggested that hesperetin pretreatment increased the sensitivity of A549/DDP cells to DDP.

The mechanism of drug resistance is a complex adaptive process (39,40), and one of the methods by which it manifests is by reducing the accumulation and toxicity of chemotherapeutic drugs in cells by upregulating the expression levels of the proteins that pump these drugs out of the cell or detoxify the drugs, such as P-gp and GST- π (41,42). Mechanistically, hesperetin treatment resulted in the downregulation of the MDR-associated protein P-gp, whereas the expression levels of c-erbB-2 and GST- π did not differ significantly. Additionally, previous studies demonstrated that, when the NF- κB signaling pathway was activated, p65 was phosphorylated and translocated into the nucleus, initiating the transcription of P-gp. Conversely, inhibition of p65 expression or its phosphorylation reduces the transcription levels of P-gp (43,44). In the present study, the downregulation of P-gp expression induced by hesperetin resulted in inhibition of the phosphorylation of p65,

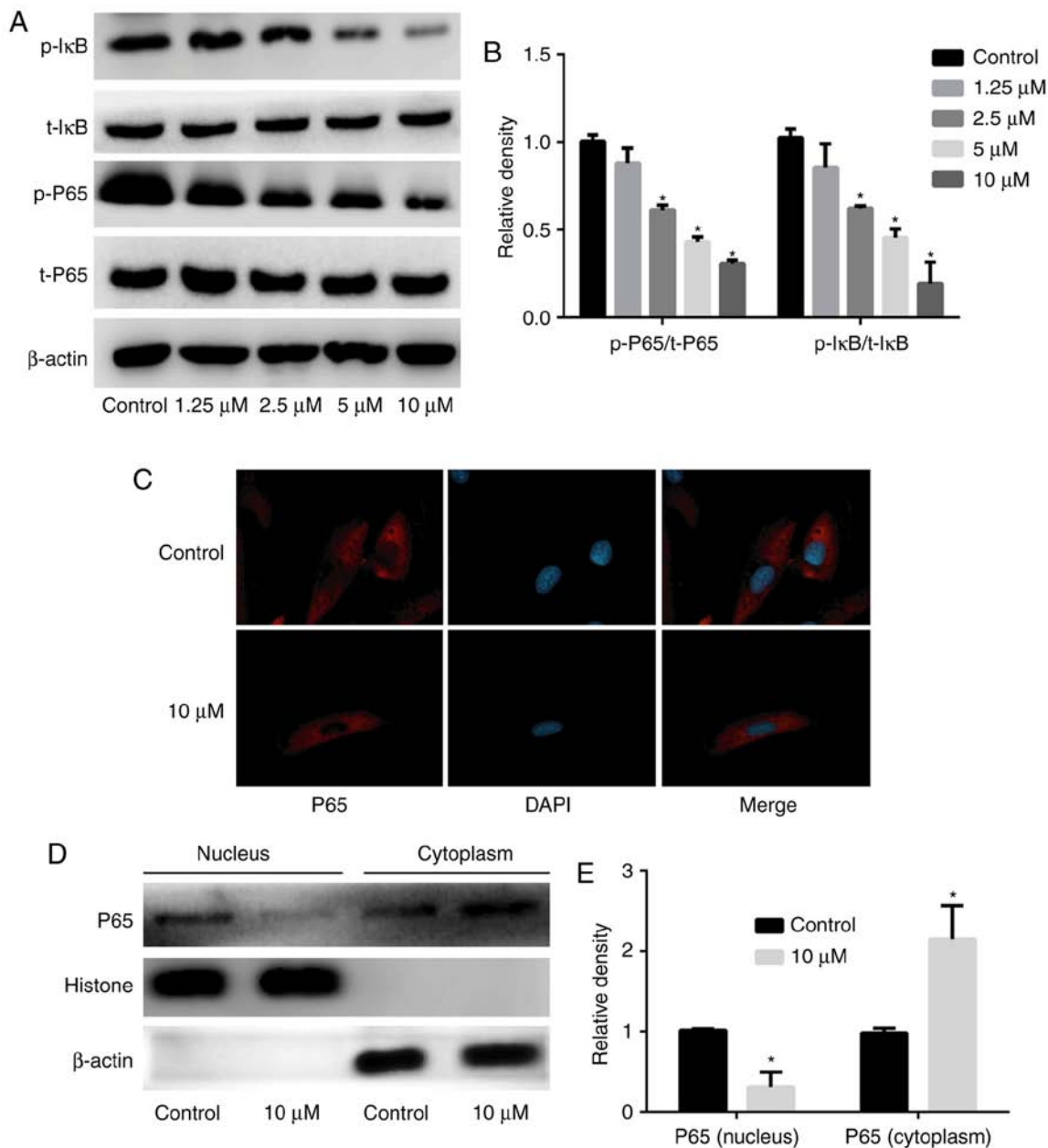


Figure 6. Hesperetin treatment reduces the activation of the nuclear factor- κ B signaling pathway. (A) Treatment with different concentrations of hesperetin resulted in downregulation of the expression of p-p65 and p-I κ B, but exerted no significant effect on the expression of t-p65 and t-I κ B. (B) Densitometry analysis of the western blots. (C) Representative images from immunofluorescence analysis. Hesperetin treatment significantly reduced the nuclear translocation of p65. Magnification, x200. (D) Representative blots of nuclear and cytoplasmic expression of P65. (E) Densitometry analysis of the p65 expression. When A549/DDP cells were treated with 10 μ M hesperetin, the levels of p65 were significantly increased in the cytoplasm and significantly decreased in the nucleus. * P <0.05 vs. control. Error bars indicate standard deviations. n=3. p-, phospho; t-, total.

thus preventing its translocation to the nucleus to exert its transcription factor effects. The effect of hesperetin on rhodamine accumulation in A549/DDP cells was determined using a rhodamine efflux assay, a suitable research model for studying intracellular drug accumulation (45,46). Rhodamine 123 accumulation was found to be lower in A549/DDP cells (lower fluorescence values) in the absence of hesperetin, whereas hesperetin pretreatment significantly increased the accumulation of rhodamine 123, suggesting that hesperetin enhanced the sensitivity of A549/DDP cells to DDP.

The results of the present study demonstrated that hesperetin downregulated the expression of P-gp by inhibiting the activation of the NF- κ B signaling pathway, thereby increasing

the accumulation of chemotherapeutic drugs in tumor cells and enhancing the toxic effects on cancer cells. Therefore, cells were treated with the NF- κ B signaling pathway inhibitor JSH-23, which specifically inhibits translocation of p65 into the nucleus (47,48). The results demonstrated that JSH-23 treatment significantly enhanced the toxic effects of DDP on A549/DDP cells by decreasing its IC_{50} concentration. When the cells were pretreated with JSH-23 and hesperetin in combination, the toxic effects of DDP on A549/DDP cells were significantly increased compared with those in cells treated with JSH-23 or hesperetin alone. Furthermore, compared with the group pretreated with JSH-23 or hesperetin alone, co-treatment of cells with JSH-23 and hesperetin significantly

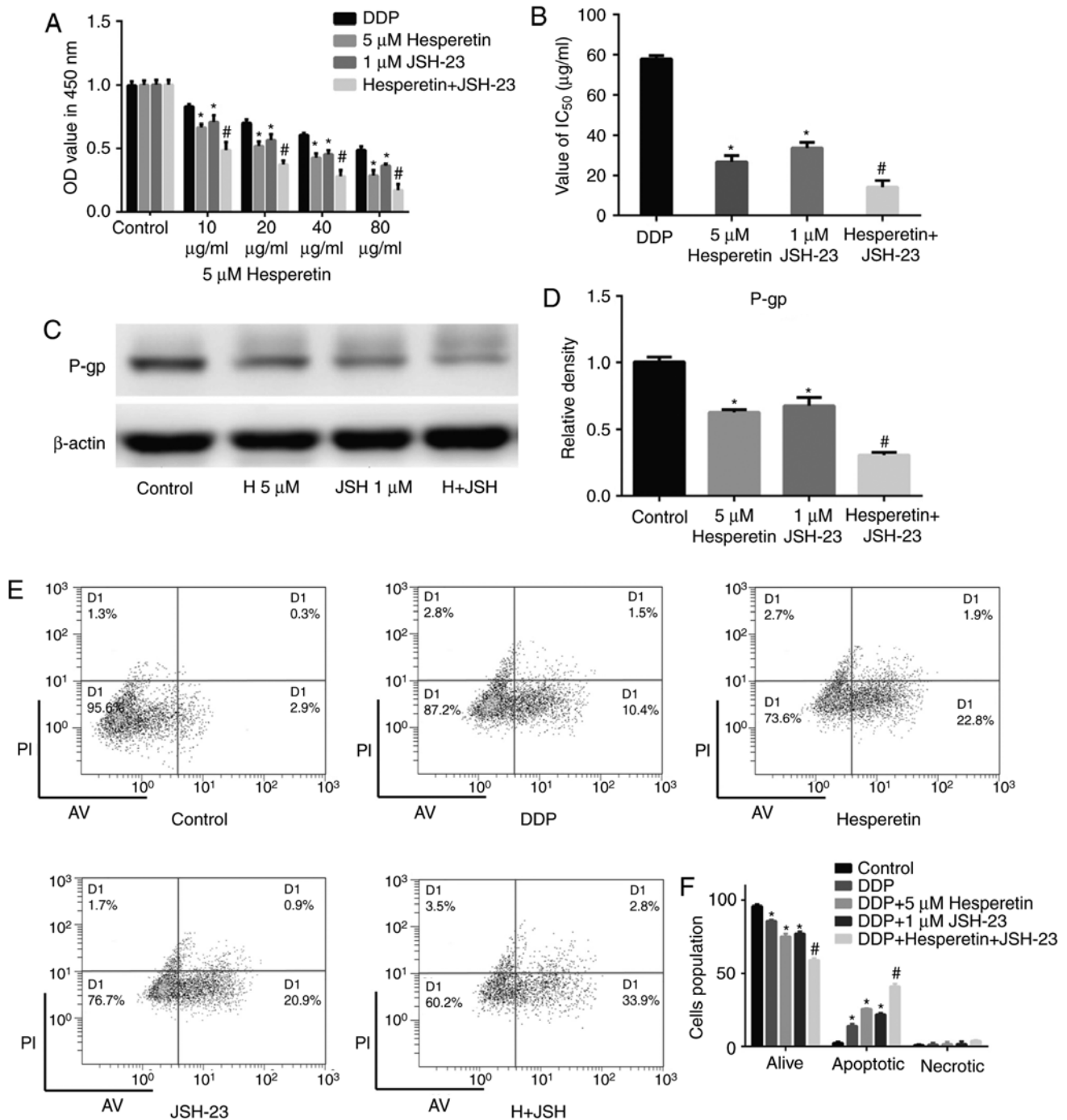


Figure 7. Hesperetin combined with the nuclear factor- κ B signaling pathway inhibitor JSH-23 significantly enhanced the sensitivity of A549/DDP cells to DDP. (A) Compared with cells treated with hesperetin or JSH-23 alone, co-treatment with hesperetin and JSH-23 significantly improved the effect of DDP on A549/DDP cells. (B) IC_{50} values of DDP on cells treated with hesperetin alone or in combination with JSH-23. IC_{50} values were significantly reduced when the treatments were combined. (C) Representative blots and (D) densitometry analysis of P-gp protein expression when A549/DDP cells were treated with hesperetin alone or combined with JSH-23. (E) Representative dot plots of apoptosis when A549/DDP cells were treated with hesperetin alone or combined with JSH-23. (F) Quantification of cell apoptosis. * $P < 0.05$ vs. control group. # $P < 0.05$ vs. hesperetin or JSH-23. Error bars indicate standard deviations. $n = 3$. H, hesperetin; DDP, cisplatin; IC_{50} , half-maximal inhibitory concentration; OD, optical density; AVG, Annexin V; PI, propidium iodide.

decreased the expression of P-gp and significantly increased apoptosis, suggesting that hesperetin enhanced the chemosensitivity of drug-resistant cells when used in combination with other drugs.

Taken together, the results suggested that hesperetin increases the sensitivity of lung cancer A549/DDP cells to DDP through downregulation of the phosphorylation of I κ B, thus inhibiting the phosphorylation of p65 and its translocation

to the nucleus and reducing the transcription and translation of P-gp. Hesperetin sensitized tumor cells to chemotherapeutic drugs, providing a theoretical basis for its application as an adjuvant treatment in the clinical setting.

Acknowledgements

Not applicable.

Funding

The present study was supported in part by Joint Funds for the Innovation of Science and Technology from Fujian Province (grant no. 2017Y9127).

Availability of data and materials

The datasets used and/or analyzed during the current study are available from the corresponding author on reasonable request.

Authors' contributions

WK and ZY wrote the manuscript; ZY and GL designed and supervised the study; WK, XL, YC, XW, ZZ, WW and SW performed the experiments; WK, XL and YC analyzed and interpreted the experimental data; all the authors discussed the results and commented on the manuscript. All authors read and approved the final manuscript.

Ethics approval and consent to participate

All mouse experiments were approved by the Animal Care and Use Committee of 900 Hospital of the Joint Logistics Team and carried out in accordance with the Guide for the Care and Use of Laboratory Animals.

Patient consent for publication

Not applicable.

Competing interests

The authors declare that there have no competing interests.

References

- Siegel RL, Miller KD and Jemal A: Cancer Statistics, 2017. *CA Cancer J Clin* 67: 7-30, 2017.
- Girard L, Rodriguez-Canales J, Behrens C, Thompson DM, Botros IW, Tang H, Xie Y, Rekhman N, Travis WD, Wistuba II, *et al*: An expression signature as an aid to the histologic classification of non-small cell lung cancer. *Clin Cancer Res* 22: 4880-4889, 2016.
- Nizzoli R, Tiseo M, Gelsomino F, Bartolotti M, Majori M, Ferrari L, De Filippo M, Rindi G, Silini EM, Guazzi A and Ardizzoni A: Accuracy of fine needle aspiration cytology in the pathological typing of non-small cell lung cancer. *J Thorac Oncol* 6: 489-493, 2011.
- Osmani L, Askin F, Gabrielson E and Li QK: Current WHO guidelines and the critical role of immunohistochemical markers in the subclassification of non-small cell lung carcinoma (NSCLC): Moving from targeted therapy to immunotherapy. *Semin Cancer Biol* 52: 103-109, 2018.
- Watanabe SI, Nakagawa K, Suzuki K, Takamochi K, Ito H, Okami J, Aokage K, Saji H, Yoshioka H, Zenke Y, *et al*: Neoadjuvant and adjuvant therapy for Stage III non-small cell lung cancer. *Jpn J Clin Oncol* 47: 1112-1118, 2017.
- Pöttgen C, Eberhardt W, Stamatidis G and Stuschke M: Definitive radiochemotherapy versus surgery within multimodality treatment in stage III non-small cell lung cancer (NSCLC)-a cumulative meta-analysis of the randomized evidence. *Oncotarget* 8: 41670-41678, 2017.
- Masters GA, Temin S, Azzoli CG, Giaccone G, Baker S Jr, Brahmer JR, Ellis PM, Gajra A, Rackear N, Schiller JH, *et al*: Systemic therapy for stage IV non-small-cell lung cancer: American society of clinical oncology clinical practice guideline update. *J Clin Oncol* 33: 3488-3515, 2015.
- Rancoule C, Guy JB, Vallard A, Ben Mrad M, Rehailla A and Magné N: (50th anniversary of cisplatin). *Bull Cancer* 104: 167-176, 2017 (In French).
- Dasari S and Tchounwou PB: Cisplatin in cancer therapy: Molecular mechanisms of action. *Eur J Pharmacol* 740: 364-378, 2014.
- Zhang K, Wang X and Wang H: Effect and mechanism of Src tyrosine kinase inhibitor sunitinib on the drug-resistance reversal of human A549/DDP cisplatin-resistant lung cancer cell line. *Mol Med Rep* 10: 2065-2072, 2014.
- Yao C, Jiang J, Tu Y, Ye S, Du H and Zhang Y: β -elemene reverses the drug resistance of A549/DDP lung cancer cells by activating intracellular redox system, decreasing mitochondrial membrane potential and P-glycoprotein expression, and inducing apoptosis. *Thorac Cancer* 5: 304-312, 2014.
- Lv J and Tian Y: Effect of Src tyrosine kinase inhibition on the drug-resistance as well as MDR1 and LRP expression of the human cis-platinum-resistant lung cancer cell line A549/DDP. *Zhongguo Fei Ai Za Zhi* 15: 501-506, 2012 (In Chinese).
- Zhong Y, Lee K, Deng Y, Ma Y, Chen Y, Li X, Wei C, Yang S, Wang T, Wong NJ, *et al*: Arctigenin attenuates diabetic kidney disease through the activation of PP2A in podocytes. *Nat Commun* 10: 4523, 2019.
- Wagner L, Cramer H, Klose P, Lauche R, Gass F, Dobos G and Langhorst J: Herbal medicine for cough: A systematic review and meta-analysis. *Forsch Komplementmed* 22: 359-368, 2015.
- Wong YK, Xu C, Kalesh KA, He Y, Lin Q, Wong WSF, Shen HM and Wang J: Artemisinin as an anticancer drug: Recent advances in target profiling and mechanisms of action. *Med Res Rev* 37: 1492-1517, 2017.
- Safarzadeh E, Sandoghchian Shotorbani S and Baradaran B: Herbal medicine as inducers of apoptosis in cancer treatment. *Adv Pharm Bull* 4(Suppl 1): 421-427, 2014.
- Roohbakhsh A, Parhiz H, Soltani F, Rezaee R and Iranshahi M: Molecular mechanisms behind the biological effects of hesperidin and hesperetin for the prevention of cancer and cardiovascular diseases. *Life Sci* 124: 64-74, 2015.
- Xia R, Sheng X, Xu X, Yu C and Lu H: Hesperidin induces apoptosis and G0/G1 arrest in human non-small cell lung cancer A549 cells. *Int J Mol Med* 41: 464-472, 2018.
- Xia R, Xu G, Huang Y, Sheng X, Xu X and Lu H: Hesperidin suppresses the migration and invasion of non-small cell lung cancer cells by inhibiting the SDF-1/CXCR-4 pathway. *Life Sci* 201: 111-120, 2018.
- Bodduluru LN, Kasala ER, Barua CC, Karnam KC, Dahiya V and Ellutla M: Antiproliferative and antioxidant potential of hesperetin against benzo(a)pyrene-induced lung carcinogenesis in Swiss albino mice. *Chem Biol Interact* 242: 345-352, 2015.
- Kamaraj S, Anandakumar P, Jagan S, Ramakrishnan G and Devaki T: Modulatory effect of hesperidin on benzo(a)pyrene induced experimental lung carcinogenesis with reference to COX-2, MMP-2 and MMP-9. *Eur J Pharmacol* 649: 320-327, 2010.
- Kamaraj S, Anandakumar P, Jagan S, Ramakrishnan G and Devaki T: Hesperidin attenuates mitochondrial dysfunction during benzo(a)pyrene-induced lung carcinogenesis in mice. *Fundam Clin Pharmacol* 25: 91-98, 2011.
- Kamaraj S, Ramakrishnan G, Anandakumar P, Jagan S and Devaki T: Antioxidant and anticancer efficacy of hesperidin in benzo(a)pyrene induced lung carcinogenesis in mice. *Invest New Drugs* 27: 214-222, 2009.
- Wolfram J, Scott B, Boom K, Shen J, Borsoi C, Suri K, Grande R, Fresta M, Celia C, Zhao Y, *et al*: Hesperetin liposomes for cancer therapy. *Curr Drug Deliv* 13: 711-719, 2016.
- El Daibani AA, Xi Y, Luo L, Mei X, Zhou C, Yasuda S and Liu MC: Sulfation of hesperetin, naringenin and apigenin by the human cytosolic sulfotransferases: A comprehensive analysis. *Nat Prod Res* 6: 1-7, 2018.
- Aranganathan S and Nalini N: Efficacy of the potential chemopreventive agent, hesperetin (citrus flavanone), on 1,2-dimethylhydrazine induced colon carcinogenesis. *Food Chem Toxicol* 47: 2594-2600, 2009.
- Sivagami G, Vinothkumar R, Bernini R, Preethy CP, Riyasdeen A, Akbarsha MA, Menon VP and Nalini N: Role of hesperetin (a natural flavonoid) and its analogue on apoptosis in HT-29 human colon adenocarcinoma cell line-a comparative study. *Food Chem Toxicol* 50: 660-671, 2012.
- Livak KJ and Schmittgen TD: Analysis of relative gene expression data using real-time quantitative PCR and the 2^{-Delta Delta} C(T) method. *Methods* 25: 402-408, 2001.

29. Heist RS: First-line systemic therapy for non-small cell lung cancer. *Hematol Oncol Clin North Am* 31: 59-70, 2017.
30. Zhang XW, Liu W, Jiang HL and Mao B: Chinese herbal medicine for advanced non-small-cell lung cancer: A systematic review and meta-analysis. *Am J Chin Med* 46: 923-952, 2018.
31. Li TM, Yu YH, Tsai FJ, Cheng CF, Wu YC, Ho TJ, Liu X, Tsang H, Lin TH, Liao CC, *et al*: Characteristics of Chinese herbal medicine usage and its effect on survival of lung cancer patients in Taiwan. *J Ethnopharmacol* 213: 92-100, 2018.
32. Byun EB, Kim HM, Song HY and Kim WS: Hesperidin structurally modified by gamma irradiation induces apoptosis in murine melanoma B16BL6 cells and inhibits both subcutaneous tumor growth and metastasis in C57BL/6 mice. *Food Chem Toxicol* 127: 19-30, 2019.
33. Elango R, Athinarayanan J, Subbarayan VP, Lei DKY and Alshatwi AA: Hesperetin induces an apoptosis-triggered extrinsic pathway and a p53-independent pathway in human lung cancer H522 cells. *J Asian Nat Prod Res* 20: 559-569, 2018.
34. Chen X, Wei W, Li Y, Huang J and Ci X: Hesperetin relieves cisplatin-induced acute kidney injury by mitigating oxidative stress, inflammation and apoptosis. *Chem Biol Interact* 308: 269-278, 2019.
35. Li Q, Miao Z, Wang R, Yang J and Zhang D: Hesperetin induces apoptosis in human glioblastoma cells via p38 MAPK activation. *Nutr Cancer* Jul 11, 2019 (Epub ahead of print).
36. Shokri Afra H, Zangoeei M, Meshkani R, Ghahremani MH, Ilbeigi D, Khedri A, Shahmohamadnejad S, Khaghani S and Nourbakhsh M: Hesperetin is a potent bioactivator that activates SIRT1-AMPK signaling pathway in HepG2 cells. *J Physiol Biochem* 75: 125-133, 2019.
37. Mary Lazer L, Sadhasivam B, Palaniyandi K, Muthuswamy T, Ramachandran I, Balakrishnan A, Pathak S, Narayan S and Ramalingam S: Chitosan-based nano-formulation enhances the anticancer efficacy of hesperetin. *Int J Biol Macromol* 107: 1988-1998, 2018.
38. Li WX, Chen X, Yang Y, Huang HM, Li HD, Huang C, Meng XM and Li J: Hesperitin derivative-11 suppress hepatic stellate cell activation and proliferation by targeting PTEN/AKT pathway. *Toxicology* 381: 75-86, 2017.
39. Zheng HC: The molecular mechanisms of chemoresistance in cancers. *Oncotarget* 8: 59950-59964, 2017.
40. Senthebane DA, Rowe A, Thomford NE, Shipanga H, Munro D, Mazeedi MAMA, Almazaydi HAM, Kallmeyer K, Dandara C, Pepper MS, *et al*: The role of tumor microenvironment in chemoresistance: To survive, keep your enemies closer. *Int J Mol Sci* 18: E1586, 2017.
41. Cavaco MC, Pereira C, Kreutzer B, Gouveia LF, Silva-Lima B, Brito AM and Videira M: Evading P-glycoprotein mediated-efflux chemoresistance using solid lipid nanoparticles. *Eur J Pharm Biopharm* 110: 76-84, 2017.
42. Hermawan A, Wagner E and Roidl A: Consecutive salinomycin treatment reduces doxorubicin resistance of breast tumor cells by diminishing drug efflux pump expression and activity. *Oncol Rep* 35: 1732-1740, 2016.
43. Feng Q, Yang W, Gao Z, Ruan X and Zhang Y: Up-regulation of P-gp via NF-kB activation confers protection against oxidative damage in the retinal pigment epithelium cells. *Exp Eye Res* 181: 367-373, 2019.
44. Shi Y, Wang SY, Yao M, Sai WL, Wu W, Yang JL, Cai Y, Zheng WJ and Yao DF: Chemosensitization of HepG2 cells by suppression of NF-kappaB/p65 gene transcription with specific-siRNA. *World J Gastroenterol* 21: 12814-12821, 2015.
45. Kim M, Cooper DD, Hayes SF and Spangrude GJ: Rhodamine-123 staining in hematopoietic stem cells of young mice indicates mitochondrial activation rather than dye efflux. *Blood* 91: 4106-4117, 1998.
46. Jancis EM, Chen HX, Carbone R, Hochberg RB and Dannies PS: Rapid stimulation of rhodamine 123 efflux from multidrug-resistant KB cells by progesterone. *Biochem Pharmacol* 46: 1613-1619, 1993.
47. Wang Q, Dong X, Li N, Wang Y, Guan X, Lin Y, Kang J, Zhang X, Zhang Y, Li X and Xu T: JSH-23 prevents depressive-like behaviors in mice subjected to chronic mild stress: Effects on inflammation and antioxidant defense in the hippocampus. *Pharmacol Biochem Behav* 169: 59-66, 2018.
48. Kumar A, Negi G and Sharma SS: JSH-23 targets nuclear factor-kappa B and reverses various deficits in experimental diabetic neuropathy: Effect on neuroinflammation and antioxidant defence. *Diabetes Obes Metab* 13: 750-758, 2011.



This work is licensed under a Creative Commons Attribution-NonCommercial-NoDerivatives 4.0 International (CC BY-NC-ND 4.0) License.